U-Pb geochronology and Hf isotopes of the Grenvillian Río Hondo gneisses, Puebla: Redefining the western edge of Oaxaquia

Luigi A. Solari[1,*], Mariano Elías-Herrera[2], Guillermo Espejo-Bautista[1], Mariana Jaramillo-Jaramillo[1], María del Consuelo Macías-Romo[2], and Carlos Ortega-Obregón[1]

[1] Instituto de Geociencias, Universidad Nacional Autónoma de México, Campus Juriquilla, 76230 Juriquilla, Querétaro (QRO), Mexico.

[2] Instituto de Geología, Universidad Nacional Autónoma de México, Ciudad Universitaria, 04510 Del. Coyoacán, Mexico City, Mexico.

*solari@unam.mx

ABSTRACT

In situ Río Hondo (Puebla, southern Mexico) gneiss samples, as well as clastic samples recovered from the nearby-outcropping latest Paleozoic Matzitzi Formation, a fluvial unit mainly sourced by Grenvillian rocks, were historically interpreted as representative of the northernmost exposures of the Oaxacan Complex, the largest outcrop of ortho and metasedimentary units, made up of mostly 1.0–1.3 Ga protoliths, affected cfby local migmatization (*ca.* 1.1 Ga) and granulite facies metamorphism at *ca.* 0.98 Ga, constituting the most prominent outcrop of the Oaxaquia microcontinent.

U-Pb geochronology and Lu-Hf isotopic determinations in zircon by LA-(MC)-ICP-MS were performed on both in situ and clast samples. *In situ* basement samples record a *ca.* 1.2 crystallization event, together with a younger one at *ca.* 1.02 Ga. both lacking inherited >1.3 Ga components. The clasts have an unimodal zircon U-Pb age distribution, recording a crystallization event at *ca.* 1.2–1.27 Ga. Scarce inherited zircon cores between *ca.* 1.4–1.6 Ga were found, with only a few samples with a broader age distribution, suggesting a detrital protolith with zircon cores as old as *ca.* 1.8 and 2.4 Ga. No zircon overgrowths or geochemical-petrographic evidences are indicative of granulite metamorphism. Furthermore, all the studied metaigneous samples show discordant zircon ages produced by Pb loss events barely constrained between the latest Paleozoic to the Mesozoic.

Hf isotopes reveal that zircon crystals from clasts have a range of εHf $_{(1.25 \, Ga)}$ ≈+1 to +5 and yield Hf model ages from 1.7 to 1.9 Ga. On the other hand, the The zircon Hf isotopes of one analyzed basement sample reveal a higher range of εHf $_{(1.25 \, Ga)}$ ≈+7 to +9, and Hf model ages from 1.5 to 1.6 Ga.

Both ≈1.2 Ga and 1.02 Ga events are consistent with magmatic ages previously documented elsewhere in Oaxaquia, interpreted as indicating portions of the NW Amazonia-Oaxaquia arc system with cratonic influence or to slices of Baltica thrust over Oaxaquia during the Grenville orogeny. However, the absence of granulite facies indicators, such as zircon metamorphic ages and/or granulite paragenesis (typically, in other Oaxaquia samples, orthopyroxene and garnet) are interpreted as prime evidence that the studied samples didn't undergo such high grade of metamorphism. Río Hondo gneisses, as this sequence is informally named, must belong to a source that had the influence of an older continental crust and can be tentatively associated either with rocks recently described in the Sierra de Juárez, or those belonging to the central basement of the Maya block, currently exposed farther to the SE in Chiapas.

Keywords: Grenville orogen; Oaxacan Complex; Mexico; U-Pb geochronology; Hf isotopes.

RESUMEN

Muestras de gneis in situ (Río Hondo, Puebla, México) y clastos recuperados de la Formación Matzitzi del Paleozoico tardío, una unidad fluvial originada principalmente por la erosión y depósito de unidades grenvillianas, se han interpretado históricamente como representativas de la porción más septentrional del Complejo Oaxaqueño, el afloramiento más grande de unidades orto y metasedimentarias de 1.0–1.3 Ga, afectados por migmatización local (ca. 1.1 Ga) y metamorfismo de facies de granulita en ca. 0.98 Ga, interpretados como el núcleo del microcontinente Oaxaquia.

Se realizaron determinaciones geocronológicas de U-Pb e isotópicas de Lu-Hf en circón mediante LA-(MC)-ICP-MS. , Las muestras de basamento colectadas in situ registran el evento de cristalización de ca. 1.2 Ga, junto con uno más joven en ca. 1.02 Ga. Sin embargo, carecen de componentes heredados > 1.3 Ga. La mayoría de los clastos estudiados tienen una distribución de edades U-Pb de circón unimodal, registrándose un evento de cristalización a ca. 1.2–1.27 Ga. Escasos núcleos de circón

heredados, entre ca 1.4–1.6 Ga se han encontrado, con solo unas pocas muestras con una distribución de edad más amplia, intepretadas como un protolito detrítico con núcleos de circón tan antiguo como ca. 1.8 y 2.4 Ga. Las observaciones petrográficas, así como la geoquímica de zircones, no evidencian la existencia de sobrecrecimientos de circón indicativo de metamorfismo de granulita. Además, todas las muestras metaígneas estudiadas muestran edades de circón discordantes producidas por eventos de pérdida de Pb no bien identificados, pero que ocurrieron entre el Paleozoico tardío y el Mesozoico.

Los isótopos de Hf revelan que los cristales de circón de los clastos tienen un rango de εHf (1.25 Ga) ≈+1 a +5 y producen edades modelo de Hf de 1.7 a 1.9 Ga. Por otro lado los isótopos de Hf de una muestra de basamento in situ analizada revelan un rango más alto de εHf (1.25 Ga) ≈+7 a +9, correspondiendo con edades modelo de 1.5 a 1.6 Ga.

Ambos eventos de ≈1.2 Ga y 1.02 Ga son consistentes con edades magmáticas previamente documentadas en otras partes del Complejo Oaxaqueño y, más en general, Oaxaquia, interpretadas como indicativas de porciones del sistema de arco NW de Amazonia-Oaxaquia con influencia cratónica, o bien, fragmentos de Baltica cabalgados arriba de Oaxaquia durante la orogenia Grenville. Sin embargo, la ausencia de indicadores de facies de granulita, como edades metamórficas de circón y/o paragénesis de granulita (típicamente, en otras muestras de Oaxaquia, ortopiroxeno y granate) indican que las muestras estudiadas no sufrieron un grado tan alto de metamorfismo. Los gneises de Río Hondo, como se denomina informalmente a esta secuencia, deben pertenecer a una fuente que tuvo la influencia de una corteza continental más antigua y se pueden asociar tentativamente con unidades de la Sierra de Juárez o con el basamento central del bloque Maya, actualmente expuesto más al SE en Chiapas.

INTRODUCTION

The *ca.* 0.95–1.3 Ga Grenville orogen is one of the most studied and complete tectonic systems that originated during the Proterozoic. It is the result of the amalgamation of the supercontinent Rodinia, originated by the convergence of Laurentia, Baltica, and Amazonia (Li *et al.*, 2008; Cawood *et al.*, 2013).

Mexico is considered the site of a significant portion of such basement, which constitutes the *ca.* 0.95–1.3 Ga, N-S framework of the microcontinent Oaxaquia (*e.g.*, Ortega-Gutiérrez *et al.*, 1995; Ortega-Gutiérrez *et al.*, 2018). While such units crop out discontinuously along the Mexican territory, the Oaxacan Complex (OC) exposed in southern Mexico constitutes the most extensive and continuous outcrop of approximately 7000 km² (Figure 1). Several papers in the last two decades documented the tectonic history of the OC basement rocks, primarily using geochronology and isotopic techniques (*e.g.*, Keppie *et al.*, 2001 and 2003; Solari *et al.*, 2003, 2004, 2014 and 2021; Weber *et al.*, 2010; Weber and Schulze, 2014; Adame-Martínez *et al.*, 2020), mainly focusing on several localities in the Oaxaca State.

In this paper, we present new geochronology and isotopic data of a previously unstudied locality situated north of those mentioned above, in the Coatepec and Río Hondo creeks of the southern Puebla state, which constitutes the northernmost known direct outcrop of gneissic rocks south of the Quaternary Trans Mexican Volcanic Belt (Figure 1, inset). This locality is tectonically crucial because it lies exactly E of the Caltepec fault zone, a dextral transform shear system, interpreted by Elías-Herrera and Ortega-Gutiérrez (2002) and Elías-Herrera *et al.* (2005) as the tectonic, accretionary boundary between the Mixteco (Acatlán Complex) and Zapoteco (Oaxacan Complex) terranes during the mid-Permian. *In situ* samples are complemented with gneiss boulders found in the unconformable conglomerate of the late Permian-Early Triassic Matzitzi Formation (Bedoya *et al.*,
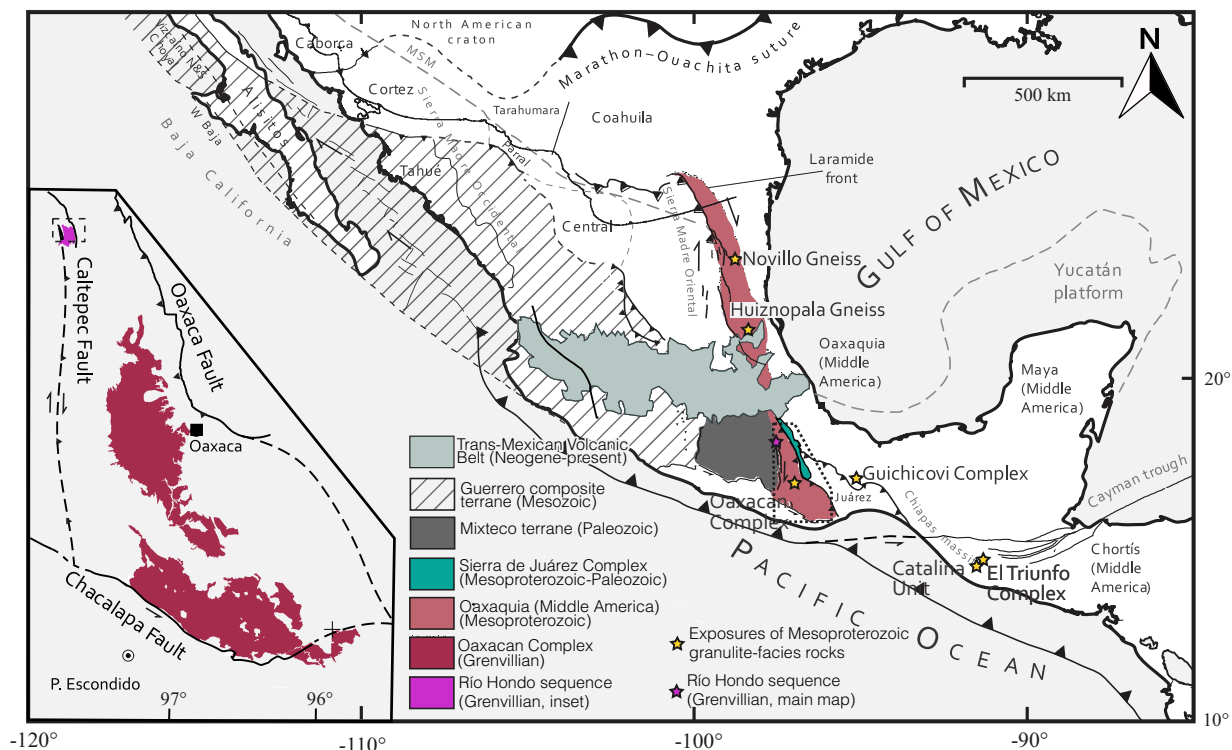

Figure 1. General map of Mexico, indicating the context of the main basement and feature outcrops. The location of the Río Hondo sequence is represented in purple color in the inset and, by a purple star, in the main Figure. Modified from Solari *et al.*, 2014.

2021; Martini *et al.*, 2022) to contribute to the study of the Proterozoic basement of southern Mexico and to refine the tectonic models in which Oaxaquia interplayed with other crustal blocks, leading to the final assembly of Rodinia.

GEOLOGIC SETTING

The studied area is located in the Coatepec Creek, in the southern Puebla state, where the latest Permian-mid Triassic fluvial Matzitzi Formation unconformably overlies a small outcrop of high-grade gneiss interpreted as belonging to the OC (Figure 2, see also Elías-Herrera *et al.*, 2005).

The OC, the most prominent outcrop of Grenvillian granulite-facies rocks in Mexico, crops out almost continuously in southern Mexico, from the central valleys of the Tehuacán-Oaxaca region, almost to the Middle America Trench nearby Pochutla (Figure 1a). Solari *et al.* (2003) defined the Zapotecan orogeny as the *ca.* 990 Ma granulite-facies metamorphism widespread not only in the OC but also throughout Oaxaquia (*ca.* 730–850 °C and 7.5 ± 1 kbar; Mora and Valley, 1985; Solari *et al.*, 2004). Before that event, several magmatic pulses were recognized: intraplate, tholeiitic anorthosite-mangerite-charnockite-granite (AMCG) magmas, dated at *ca.* 1020–1005 Ma in the northern OC (Keppie *et al.*, 2003; Keppie and Dostal, 2007), but also recognized in the Novillo Gneiss (*ca.* 1030 Ma, Cameron *et al.*, 2004), in the Huiznopala Gneiss (anorthositic gabbro dated at 1007 ± 3 Ma, Lawlor *et al.*, 1999), and in the Guichicovi complex (Weber and Kohler, 1999); *ca.* 1280–1150 Ma alkalic, intraplate gabbro, syenite and charnockite were also recognized in the OC and Huiznopala Gneiss (Lawlor *et al.*, 1999; Keppie *et al.*, 2001, 2003), as well as in the

Guichicovi Complex (*ca.* 1230 Ma, Weber and Köhler, 1999; Weber *et al.*, 2010) and the Novillo Gneiss (*ca.* 1170 Ma, Cameron *et al.*, 2004). Older magmatic pulses were also reported locally, in some of the same outcrops, with peaks at around 1.4 Ga (Weber and Schulze, 2014). Scarce granulite orthogneisses were also described as characterized by an arc-like geochemical signature, at least in the southern OC (Keppie *et al.*, 2001) and in Huiznopala (Lawlor *et al.*, 1999), thus reflecting the similar association of arc and backarc (intraplate) protoliths described by Weber and Hecht (2003) in the Guichicovi Complex.

A wealth of Hf isotopes has been published during the last decade on granulite-facies Oaxaquia rocks, pioneered by Weber *et al.* (2010) and Weber and Schulze (2014), who defined a primitive field named "typical Oaxaquia," characterized by εHf values ranging from +5 to +7, which would correspond to a marginal or oceanic arc setting, distinguishing it from a second more evolved group (primarily based on samples from the Huiznopala Gneiss), named "continental Oaxaquia" and probably allochthonous. The less evolved crustal precursor was already connected to the active continental margin of NW Amazonia during the *ca.* 1.2 Ga arc magmatism. During this time, partial melting of the different crustal precursors would have occurred and the different Hf isotopic signatures ("typical Oaxaquia", "continental Oaxaquia" or the continuum between these fields) would be attributed to varying amounts of less evolved material and recycled crustal components (Weber *et al.*, 2010; Weber and Schulze, 2014; Ibanez-Mejia *et al.*, 2015, Solari *et al.*, 2021). A more extensive database by Solari *et al.* (2021) on samples belonging to the northern OC somewhat elaborates on this concept, showing that most OC samples have εHf values constituting a continuum from moderately primitive values to more evolved ones, in which the continental Oaxaquia field constitutes an end member, whose protoliths had an estimated T_{DM} age of *ca.* 1.5–1.7 Ga.
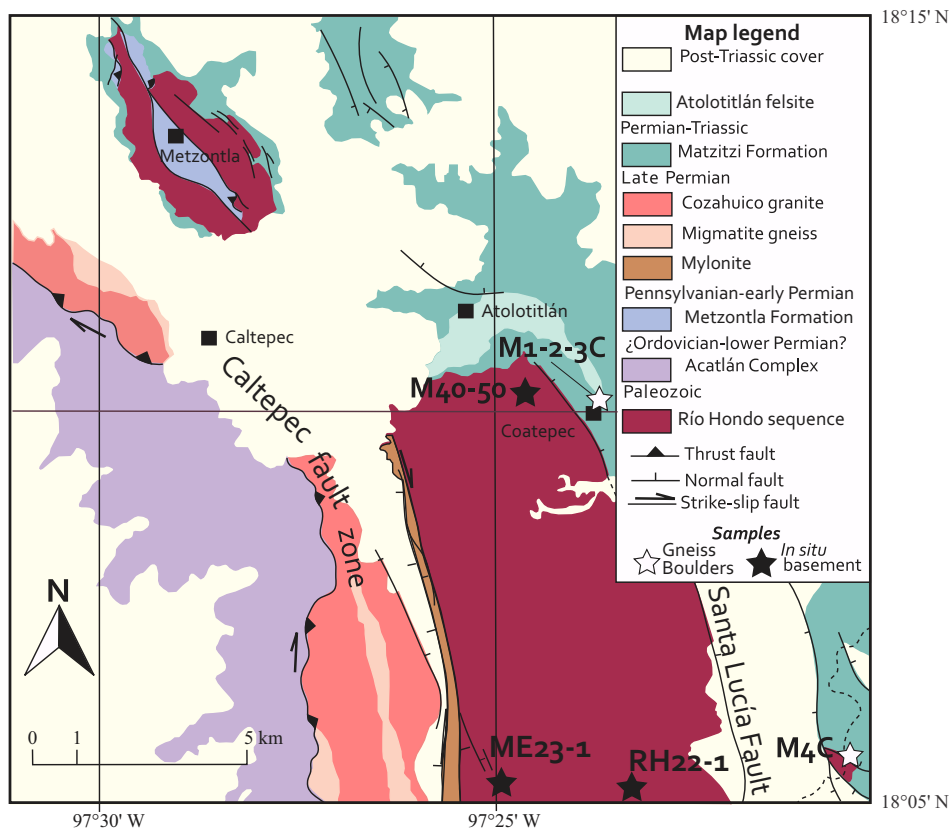

Figure 2. Geologic map of the studied area. Modified from Elías-Herrera *et al.* (2011), Juárez-Zúñiga *et al.* (2021), and Martini *et al.* (2022).

The Matzitzi Formation (Weber, 1997; Centeno-García *et al.*, 2009; Juárez-Zúñiga *et al.*, 2020; Bedoya *et al.*, 2021; Martini *et al.*, 2022) is a fluvial unit representing an anastomosing channel that was active during the latest Permian. According to the model proposed by Martini *et al.* (2022), the Matzitzi Formation was deposited during the early rifting of equatorial Pangea during the latest Permian. While it is mainly composed of coarse to medium-grained sandstone, the portion deposited just above the outcropping gneisses constitutes a very coarsely-grained conglomerate, with well-rounded boulders as large as 50 cm in diameter. The boulders consist of gneisses (the focus of this work), although volcanic (andesitic, dioritic, and rhyolitic) and granitic clasts of variable dimensions and, principally, of Permian age are also present (*e.g.*, Juárez-Zúñiga *et al.*, 2020). Some of the granitic boulders are in the age range of the nearby Cozahuico granite, *ca.* 270 Ma, associated with the Permian shearing along the dextral, transpressional Caltepec shear zone (*e.g.*, Elías-Herrera and Ortega-Gutiérrez, 2002; Elías-Herrera *et al.*, 2005).

In this work, we studied some *in situ* gneiss samples, which we called Río Hondo gneisses, and some of the gneissic boulders found in the Matzitzi conglomerate. With this strategy, we would characterize the high-grade gneisses, for which there are no available data, being the known, studied localities of the OC about 90 km farther to SSE (*e.g.*, Solari *et al.*, 2003), as well as the gneiss boulders, to determine whether they all resemble the *in situ* samples or if some of those found have distinct characteristics, in terms of mineralogy, age, and isotopy.

METHODS

After crushing, heavy minerals were concentrated from the selected samples by conventional separation techniques (*e.g.*, Solari *et al.*, 2007). Handpicking and mounting of zircon grains were performed under a binocular microscope, followed by epoxy pouring, curing, and polishing. Cathodoluminescence (CL) imaging was carried out using a luminoscope connected to a stereographic microscope to resolve internal structures, choose the spots to be analyzed, and eventually help the interpretation of the geochronological results. While the whole of the CL images is available in Jaramillo-Jaramillo (2020), one example of those images (one boulder and one in situ sample) is available as Figure 1 of the Supplementary Material.

U-Pb zircon geochronology was performed at the Laboratorio de Estudios Isotópicos (LEI), Centro de Geociencias, Universidad Nacional Autónoma de México, employing the methodology reported by Solari *et al.* (2018) by laser ablation inductively-coupled plasma mass spectrometry (LA-ICP-MS). All U-Pb analyses were obtained by coupling a Thermo ICap Qc quadrupole mass spectrometer with a Resonetics Resolution M050, 193 nm ArF excimer laser-ablation system. A 23 μm spot was employed for all U-Pb determinations, with a measured fluence of 6 J/cm2. The international standard zircon 91500 was used as the reference standard (Wiedenbeck *et al.*, 1995), whereas the Plešovice zircon (*ca.* 337 Ma; Sláma *et al.*, 2008) as the control (secondary) standard. NIST 610 synthetic glass was also used as an external standard to recalculate the elemental concentrations, employing ^{29}Si as an internal standard in zircon. The three standards were interspersed along the whole analytical sequence, repeating their measurement twice for each of the ten unknown zircon analyses. The obtained raw data were reduced offline using Iolite v. 4.1 (Paton *et al.*, 2011) and the VizualAge data reduction scheme of Petrus and Kamber (2012). The same software performed the quadratic error propagation of the standard zircon grains (91500) on the unknowns. During these analyses, the control standard yielded a mean $^{206}Pb/^{238}U$ age of 338.2 ± 1.6 Ma, in agreement with its accepted age. Concordia and mean

age diagrams were generated using IsoplotR (Vermeesch, 2018). The obtained data were filtered for discordance, removing those analyses that yielded >30 % normal and >-5 % inverse discordance. All the analyzed isotopic and elemental concentration data are available in the Supplementary Material Table S1.

Hf isotopes were measured in situ by LA-MC-ICP-MS on some of the zircon grains previously dated by U-Pb. Hf analyses were conducted using a spot of 44 μm in diameter, right on top of the 23 μm spot used for the U-Pb analyses, employing the same zircon mount washed in ultrapure water before the run session. The methodology is the same as that of Ortega-Obregón *et al.* (2014). The Neptune Plus Jet interface was used to improve sensitivity in laser mode, achieving a tuning (parameters in Table 1) optimized to maximize the Hf signal, minimize oxide formation, and avoid the formation of rare-earth element (REE) oxides (*cf.* Payne *et al.*, 2013), as well as control the mass bias. Once correctly tuned, the high sensitivity of the Neptune Plus allowed an average total Hf signal of more than 10 V (Table S2 of the Supplementary Material), a value that is similar to and, in many cases, exceeds other works with a similar setup (*e.g.*, Gerdes and Zeh, 2009; Fisher *et al.*, 2011). We avoided analyzing Hf in those zircon grains that were too small for the 44 μm spot size or those that yielded discordant U-Pb ages. Tuning was thus performed in NIST 610 standard glass, employing the same analytical conditions used during analyses (Table 1). 9–10 mL/min of N_2 was added to the He carrier gas before the plasma, to increase plasma temperature and decrease oxide formation. Compared to U-Pb laser ablation analyses, downhole fractionation is not an issue for Hf analyses, but the correction for interferences of Yb and Lu is of seminal importance (*e.g.*, Woodhead *et al.*, 2004; Hawkesworth and Kemp, 2006; Gerdes and Zeh, 2009). To correctly apply power laws and correct for those interferences, the Yb mass bias was calculated using the measured ^{172}Yb and ^{173}Yb masses and the Chu *et al.* (2002) Yb isotope abundances, together with the $^{172}Yb/^{173}Yb$ "true" ratio of 1.35274. The ^{175}Lu was also measured, but due to the absence of a second interference-free Lu isotope, the Yb mass bias was applied instead, assuming similar fractionation behavior between Yb and Lu. The $^{176}Lu/^{175}Lu$ ratio of 0.02656 was also used (Blichert-Toft and Albarède *et al.*, 1997). This type of correction allows accurate and precise results to be obtained, as demonstrated by repeated analyses of several natural standard zircon grains, commonly analyzed for Hf isotopes (Table S2 Supplementary Material), and by the repeated analyses of the synthetic zircon grains of Fisher *et al.* (2011) doped with different amounts of REEs. These synthetic zircon grains, which contain a REE range higher than terrestrial zircon crystals, were also used to include the external reproducibility and propagate it onto the internal two standard error (2SE; *i.e.*, twice the standard error of the mean, defined as in Paton *et al.*, 2011; Fisher *et al.*, 2014) measured in unknown zircon grains (*e.g.*, Fisher *et al.*, 2014). The raw data obtained with our analytical setup were processed off-line with a data reduction scheme written in Iolite, which corrects the detected interferences, normalizes against the reference zircon (synthetic zircon grains of Fisher *et al.*, 2011), and propagates the external reproducibility. The $^{179}Hf/^{177}Hf$ normalizing value of 0.7325 (Patchett and Tatsumoto, 1981) was used. The ^{176}Lu decay constant of 1.876×10^{-11} (Scherer *et al.*, 2001) and the chondritic Hf values of Bouvier *et al.* (2008) were used to calculate εHf and depleted mantle (DM) model ages (TDM). The εHf and TDM, calculated employing the chondritic and depleted mantle values, respectively, were generally considered as reflecting minimum ages for the zircon's host magma source. A second model age (TDM_C) was then calculated using a value for the average continental crust of $^{176}Lu/^{177}Hf = 0.015$ (Griffin *et al.*, 2002) to ideally project the initial εHf of zircon grains to the depleted mantle model curve and infer possible zircon sources.

Table 1. LA-ICPMS and LA-MC-ICPMS parameters employed during the analytical sessions.

Q-ICPMS		*Laser ablation workstation*	
Brand name	Thermo ICap Qc	Brand name	Resonetics
Type	Quadrupole	Model	Resolution
Forward Power	1500 W	Laser type	ArF Excimer
Ar cooling gas flow	14 l/min	Wawelength	193 nm
Ar auxiliary gas flow	~1 l/min	Pulse length	23 ns
Ar sample gas flow	~0.8 l/min	Demagnification	15x
He carrier gas flow	0.35 l/min	Fluence	~6 J/cm^2
N2 carrier gas flow	4 ml/min	Repetition rate	5 Hz

MC-ICPMS	
Brand name	Thermo Neptune Plus
Type	MC-ICPMS

Anallytical conditions, Hf isotopes	
Forward Power	1280 W
Ar cooling gas flow	14 l/min
Ar auxiliary gas flow	0.84 l/min
Ar sample gas flow	0.95 l/min
He carrier gas flow	0.7 l/min
N2 carrier gas flow	8.5 ml/min
Spot size used	44 mm
Fluence (used)	6.2 J/cm2

Acquisition parameters for Hf analyses	
Background	15 sec
Ablation time	60 sec
Washout	15 sec

Tuning ^{238}U in NIST 610 (raster at 32 mm), max sensitivity, checking the following parameters:		Tuning ^{177}Hf in NIST 610 (raster at 32 mm), max sensitivity, checking the following parameters:	
U/Th	1–1.1	U/Th	1–1.1
UO/U	<0.2 %	UO/U	< 0.2 %
ThO/Th	<1 %	ThO/Th	< 1 %
Average tuning achieved	>600 mV ^{238}U	Average tuning achieved	90–100 mV ^{177}Hf

Cup configurations

U-Pb

IC2	IC4	L4	L3	L2	H2	H4
^{201}Hg	^{204}Pb	^{206}Pb	^{207}Pb	^{208}Pb	^{232}Th	^{238}U

Hf

L4	L3	L2	L1	Ax	H1	H2	H3
^{172}Yb	^{173}Yb	^{175}Lu	^{176}Hf ^{176}Yb ^{176}Lu	^{177}Hf	^{178}Hf	^{179}Hf	^{180}Hf

Data reduction

U-Pb

Iolite v. 4	Paton *et al.*, 2011
VizualAge	Petrus and Kamber, 2012
Primary standard: 91500	Wiedenbeck *et al.*, 1995
Secondary standard: Plesovice	Slama *et al.*, 2008

Hf

Iolite v. 4		Paton *et al.*, 2011
$(^{173}$Yb/^{172}Yb$)_{true}$	0.73924	Chu *et al.*, 2002

U-Pb RESULTS

We dated four in situ samples, two collected south of Coatepec and the other two along the Río Hondo Creek, about 7 km south of Coatepec (sample locations in Figure 2). Further, 12 samples were boulders extracted from the conglomerate at the unconformity between the outcropping gneisses and the Matzitzi Fm. The petrographic characteristics of the studied samples are reported, together with the U-Pb results for each sample.

In situ samples

Sample M50 is a quartz-feldspar gneiss made up of quartz, feldspar (perthitic and microcline), plagioclase, biotite, and scarce green amphibole, frequently altered to chlorite (Figure 3a). We dated 35 zircon crystals from this sample, which yielded a concordant age distribution of *ca.* 1200–1250 Ma (Figure 4a). Several grains are discordant, probably due to Pb loss. A discordia line traced through the analyzed samples gives an upper intercept of 1237.8±8.2 Ma, interpreted as the protolith crystallization age of this sample. The lower intercept of 265.6±10.6 Ma is a possible indicator of the Pb loss time.

Sample M40 is a fine-grained granular igneous rock made up of quartz, perthite, plagioclase, and scarce opaques (Figure 3b). Secondary alteration (*e.g.*, sericite in plagioclase, calcite) accounts for post-crystallization and fluid-induced weathering processes. Thirty-five zircon grains were separated and dated. They are ovoidal to prismatic in shape, often with bi-pyramidal terminations. Most of the concordant ages cluster between *ca.* 1000 to *ca.* 1030 Ma (Figure 4b). About a third of the dated zircon show discordant ages, aligning along a discordia line that goes from an upper intercept of 1024.7±8.4 Ma, interpreted as the age of crystallization, to a poorly constrained lower
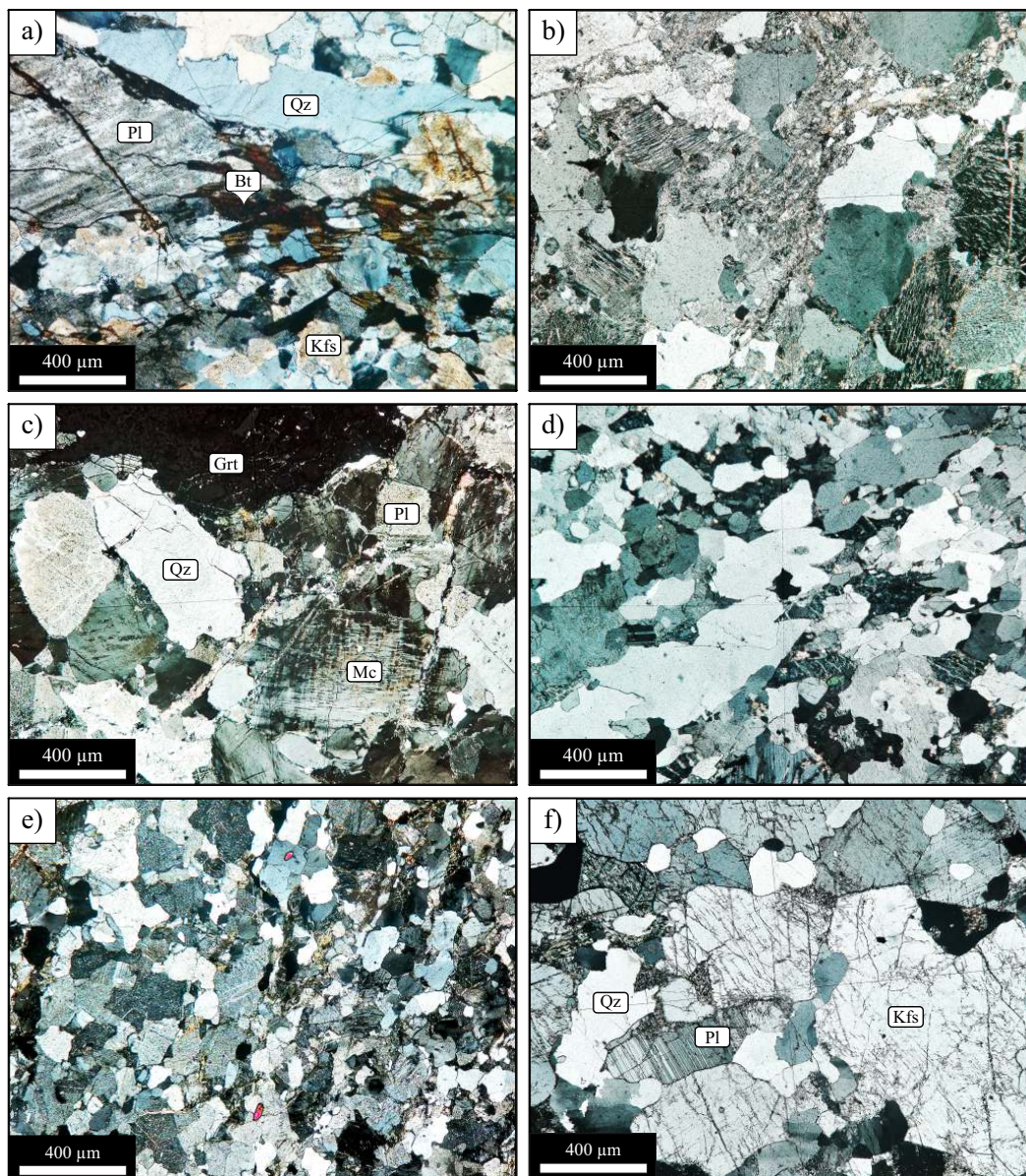

Figure 3. Photomicrographs of some selected samples: a) *In situ* sample M50. b) *In situ* sample M40. c) In-situ sample ME23-1. d) Boulder sample M4Cb consisting of an igneous rock of granitic composition. e) Boulder sample M1Ci consisting of a slightly foliated metagranitoid. f) Boulder sample M2Ca consisting of a granitoid rock with a polygonal grain arrangement.

intercept of 107.8±16.6 Ma, possibly indicating an episode of Pb loss during the Mesozoic.

Sample RH22-1 is a quartz-feldspathic gneiss collected about 5 km south of Caltepec, along Río Hondo Creek. We dated 100 spots on zircon grains separated from these samples. Most of the analyzed zircon, both core and rims, are concordant. At the same time, some are variably discordant due to Pb loss (Figure 4c). They define a discordia, with an upper intercept of 1022.4±10 Ma, interpreted as the protolith crystallization age and a poorly constrained lower intercept of *ca.* 95 Ma, indicative of a Mesozoic thermal disturbance.

Sample ME23-1 is a deformed granitoid made up of quartz, sericitized plagioclase, microcline, and it hosts poikilitic garnet, with some reaching sizes up to 4 mm (Figure 3c). This sample was collected along the Río Hondo Creek, about 1 km W of sample RH-22-1. Sixty spots were analyzed to sample the core and rims of the predominantly prismatic grains. Out of the dated grains, 58 passed the discordia filters. The resulting analyses (Figure 4d) are mostly concordant, with a group, represented mainly by core analyses, spanning between 855 to 1315 Ma (two other grains are even older, aged 1458 and 1970 Ma). A second group, mainly represented by high luminescent rims, has ages ranging between 250 and 300 Ma (Figure 4d, inset). While the Proterozoic cores probably inherited zircon grains from the protolith, the high luminescent Permian rims indicate the granite crystallization.
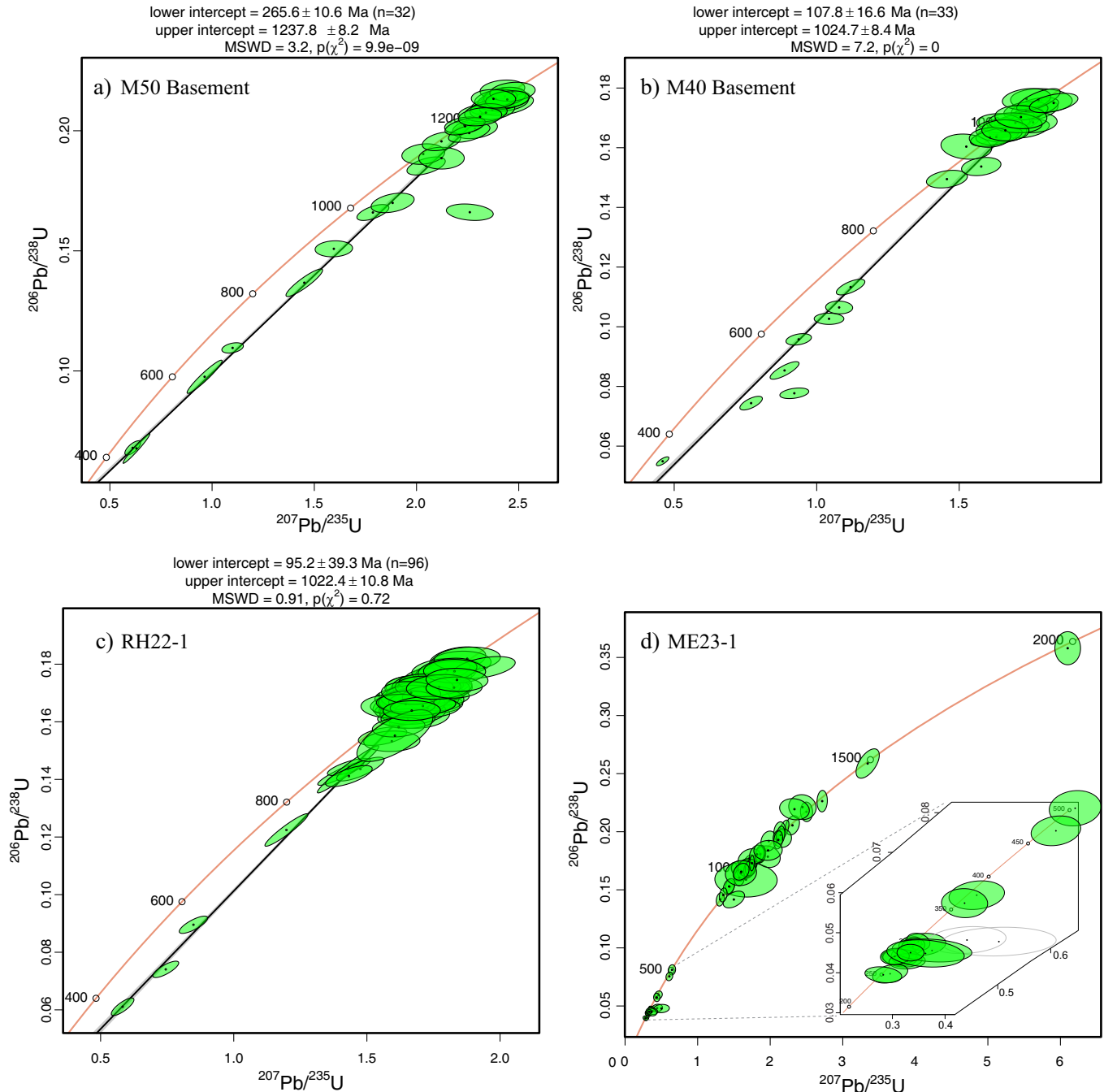

Figure 4. U-Pb geochronological data of *in situ* dated samples. All error ellipses and reported ages are at two sigma.

Boulder samples

After conducting petrographic analysis, we selected and dated 12 samples belonging to boulders collected in the conglomerate cropping out E of Coatepec at the structural bottom of the Matzitzi Formation. The selected samples are quartz-feldspathic gneisses; some have a barely foliated structure, while others have a more polygonal grain arrangement (examples in Figure 3d to 3f). In the thin section (we studied about 50 of them to choose those to be dated), only two of them had Fe-Mg bearing minerals (in one case, poikilitic garnet and, in another, 2 pyroxene grains) aside from quartz, plagioclase, feldspar (microcline and perthite), oxide minerals and accessory such as apatite, zircon, epidote, few allanite. Red biotite is sometimes observed, together with uncolored to pale-green amphibole of the second generation (after the breakdown of primary mafic minerals, impossible to distinguish).

Despite the petrographic variations, ten of the dated boulders have the same age behavior (Figure 5a to 5j), with most of the dated zircon grains concordant and some that define a variable discordia. The upper intercepts defined by concordant grains range from 1192.2±7 Ma to 1268.8±7.2 Ma, interpreted as indicative of the protolith's crystallization ages. The lower intercepts are generally poorly constrained but indicate different thermal episodes leading to Pb loss, mostly during the Mesozoic (middle Cretaceous to Late Triassic). The other two dated boulders, namely, samples M4Ca and M3Cg, are not petrographically different and are still classified as quartz-feldspar gneisses. However, they differ in the age behavior since most of the dated zircons in each are concordant but straddling the Concordia curve in a wide age range (*ca.* 920 to 1295 Ma for sample M4Ca and *ca.* 1010 to *ca.* 1800 Ma for sample M3Cg, respectively, Figure 5k and 5l). This behavior is typical of sedimentary protoliths, to which these boulders are tentatively ascribed.

Hf isotope results

Nine of the dated samples, eight belonging to boulders and one *in situ* sample, were chosen to perform Hf isotope determinations by LA-MC-ICPMS for approximately 100 analyses performed (Table S2).

εHf(t) values for each analyzed zircon were calculated concerning the depleted mantle (DM) reference values. From the DM curve, the first five εHf units were considered juvenile, the following five moderately juvenile, and the remainders evolved, indicating isotopically more evolved sources (Bahlburg *et al.*, 2011).

For all the studied zircon grains belonging to the chosen samples, the εHf(t) values, recalculated to the zircon crystallization age, fall in a restricted range limited to positive values, from +0.78 to +8.5 (Figure 6a). Only the *in situ* sample (M50) presents zircon analyses falling in the juvenile field. In contrast, all the boulder samples are moderately juvenile, with only eight analyses straddling the evolved field.

Assuming a Hf isotopic evolution similar to the average continental crust, with a ratio of $^{176}Lu/^{177}Hf = 0.015$ (*e.g.*, Griffin *et al.*, 2002, dotted lines in Figure 6), the obtained data indicate $T_{(DM)}$ ages between 1.5–1.6 Ga for the *in situ* sample M50 (U-Pb crystallization age of 1237 Ma, see above and Figure 4a), whereas the moderately juvenile studied boulders suggest a derivation from an older crustal component of a *ca.* 1.7–1.9 Ga.

ZIRCON GEOCHEMISTRY

Zircon geochemistry obtained by LA-ICPMS evidence how the totality of studied grains is suggestive of igneous crystallization, with chondrite-normalized REE plots with increasing HREE content, negative Pr and Eu anomalies as well as marked Ce and Sm ones (Figure 7).

In general, the decreasing, discordant zircon ages are accompanied by a decreasing of Yb/Gd ratio. In contrast, an increase of ΣLREE normally accompanies the decrease in ages (arrows in insets in Figure 7). This behavior is often associated to hidrothermalism or microinclusions in the analyzed zircon grains (*e.g.*, Zhong *et al.*, 2018). The igneous interpretation is also supported by the Th/U ratio (see Table S1), always >0.01, a value often taken as discriminant between zircon igneous and metamorphic crystallization (see discussion in Harley *et al.*, 2007). Sc/Yb *vs.* Nb/Yb and U/Yb *vs.* Nb/Yb tectonic discrimination diagrams (Grimes *et al.*, 2015) show how all the zircon samples fall in the continental arc domain (Figure 8a and 8b).

DISCUSSION

Age and isotopic interpretation

The combination of data presented here allows us to unravel the existence of two age groups in this basement block: the oldest of roughly 1200–1270 Ma (sample M50, *in situ*, and most of the boulder's upper intercepts), followed by a younger event at *ca.* 1022–1024 Ma (two *in situ* samples). A common feature of all those studied samples, presumably of igneous origin, is that they all show strong evidence of post-crystallization (Phanerozoic) Pb loss. On the other hand, M4Ca and M3Cg boulders, as well as the fourth studied in situ sample (meta granitoid ME23-1), present a distinct age distribution pattern, characterized by primarily concordant zircon grains, which straddle the concordia curve but are not affected by any post-crystallization Pb loss event. The Pb loss in igneous samples is sometimes poorly constrained. However, it roughly indicates events constrained from the Permian to the Mesozoic, which in principle coincide with late Paleozoic magmatism and deformation described in the area (Elías-Herrera and Ortega-Gutiérrez, 2002; Elías-Herrera *et al.*, 2005; Juárez-Zúñiga *et al.*, 2020), and tectonic reorganization during and at the end of the Gulf of Mexico opening (Bedoya *et al.*, 2021; Martini *et al.*, 2022).

While there is no doubt about the Proterozoic crystallization ages of the studied samples, there is an extensive range for their metamorphic ages. The absence of granulite facies metamorphism, as previously described in the neighboring rocks of the Oaxacan Complex (*e.g.*, Solari *et al.*, 2003 and 2014), is clear. However, it is also evident that these gneisses' metamorphism predates the Permian partial melting and mylonitization of the Cozahuico granite and deposition of the Matzitzi Fm. (*e.g.*, Elías-Herrera *et al.*, 2005 and Martini *et al.*, 2022). By comparison, two Precambrian localities of similar gneisses were recently described, with U-Pb metamorphic ages of *ca.* 940 Ma: the Catarina Unit in the Chiapas Massif Complex (Valencia-Morales *et al.*, 2022) and the Pochotepec suite in the nearby Sierra de Juárez Complex (Espejo Bautista *et al.*, 2023). It is possible that the Río Hondo gneisses shared the same metamorphic history, although at a lower metamorphic grade since the zircon grains do not show a clear metamorphic overgrowth. Alternatively, the Río Hondo gneisses could constitute a different region that didn't undergo Precambrian metamorphism and was thus only affected by a Phanerozoic event.

The obtained Hf isotope data allow comparison with similar data published for the Grenvillian rocks of Mexico (*e.g.*, Weber *et al.*, 2010; Weber and Schulze, 2014; Solari *et al.*, 2021) and NW South America (*e.g.*, Garzón, La Macarena and Guapotón Massifs in Colombia, Weber *et al.*, 2010 and Ibañez-Mejía *et al.*, 2015). In particular, the Río Hondo M50 sample is as primitive as granulite samples OC1019 and OC1015 (south of Ejutla and west of S. María Peñoles, respectively, see Solari *et al.*, 2021), which have crystallization ages of *ca.* 1350–1400 Ma. The remainder of boulders have εHf(t) values slightly more primitive than the typical Oaxaquia field of Weber *et al.* (2010), resembling the
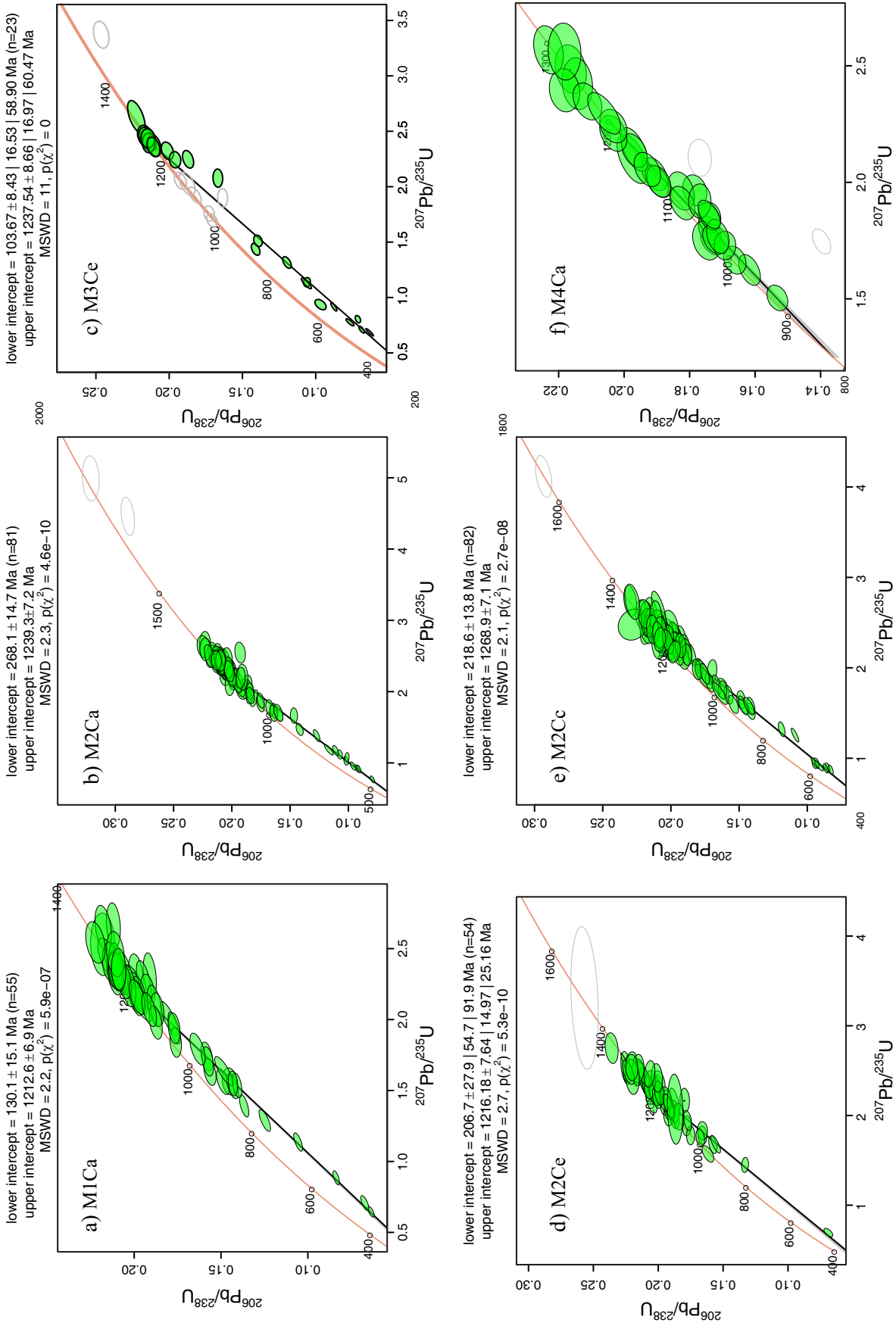
Figure 5. U-Pb geochronological data of boulder dated samples. All error ellipses and reported ages are at two sigma.
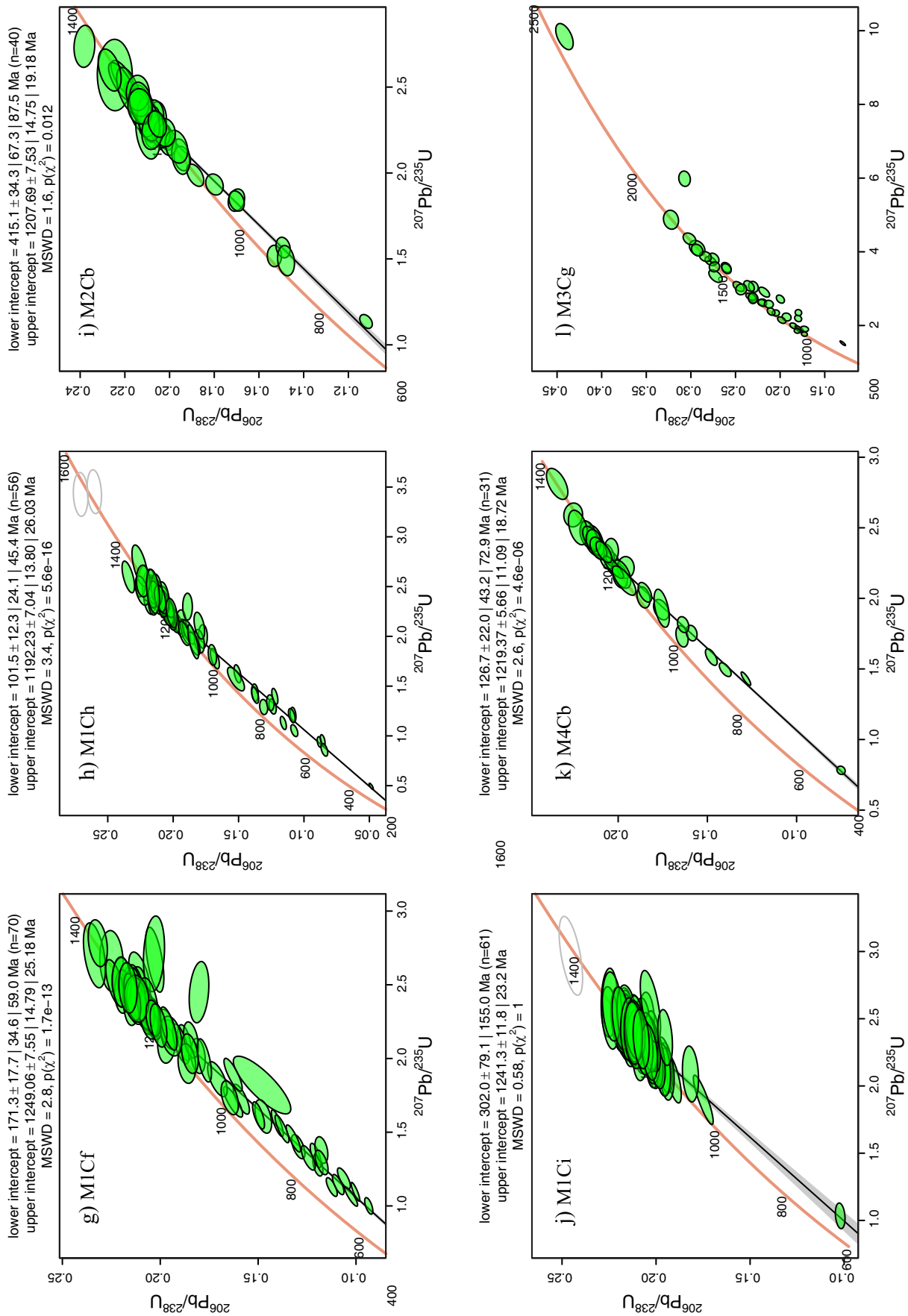
Figure 5 (cont.). U-Pb geochronological data of boulder dated samples. All error ellipses and reported ages are at two sigma.
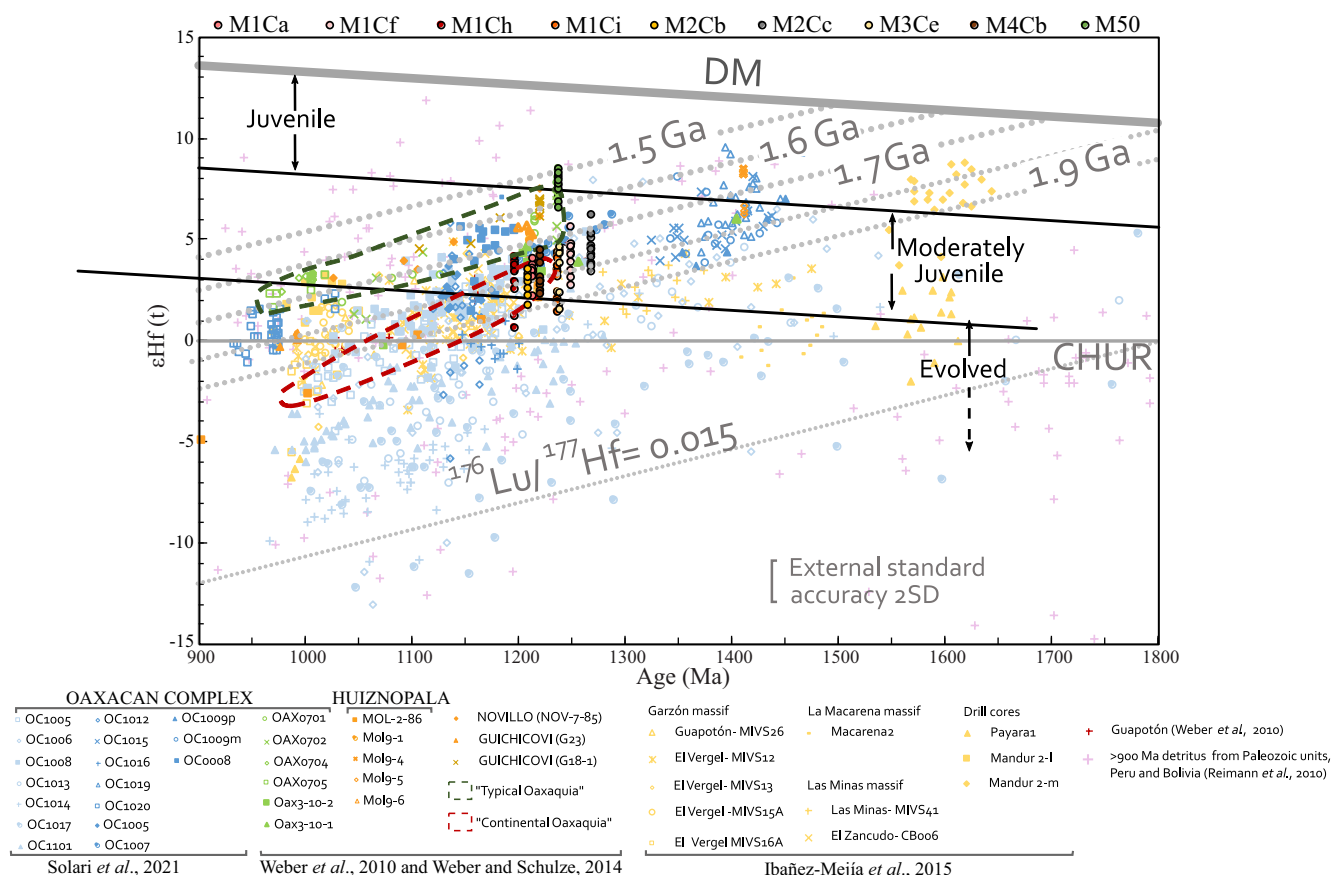
Figure 6. εHf *vs.* U–Pb calculated age, with the isotopic results obtained on the studied zircon crystals. The internal precision is generally smaller than the symbol used to plot the single analysis and is not shown to avoid the diagram cluttering. The external standard accuracy at ±2 SD (*e.g.*, Fisher *et al.* 2014), generally better than ±1ε, is reported as a comparison. The average crust evolutionary path corresponds to the ^{176}Lu/^{177}Hf value of Griffin *et al.* (2002).

values previously obtained in meta gabbro and metasyenite samples OC0008 and OC1007 by Solari *et al.* (2021). These comparisons can be applied to illustrate the similarities between the T_{DM} obtained in the Río Hondo gneiss samples, both in situ and boulders, and those calculated for the OC, between 1.5–1.65 Ga for the typical Oaxaquia, without discarding a more evolved and older crustal component for those samples yielding slightly negative εHf(t) values (*cf*. Weber *et al.*, 2010; Solari *et al.*, 2021). Similar conclusions can be extrapolated by plotting the εHf(t) values vs. the ^{176}Lu/^{177}Hf corrected values measured in zircon of the Río Hondo samples, together with those reported by Solari *et al.* (2021) for the OC samples (light brown samples in Figure 9). There is an almost complete overlap between Río Hondo and OC Hf data, reinforcing the idea that this crustal segment had a common derivation, as a mixing of a juvenile component of *ca.* 1.5–1.65 Ga, and mechanical incorporation of an even older crustal component of *ca.* 1.9 Ga, at least in some of the more evolved samples.

Tectonic implications

The calculated ages situate the main magmatic event that formed the Río Hondo sequence in two pulses that occurred in the Mesoproterozoic (*ca.* 1200–1270 and *ca.* 1025 Ma), while the sample's Hf isotopic signature suggests consanguinity with Oaxaquia rocks. The striking difference is related to the absence, in the Río Hondo samples, of granulite facies metamorphism that is always observable in the not-so-far Oaxacan Complex and, more in general, in the whole Oaxaquia outcrops. These findings imply that the Río Hondo gneisses probably belong to an external, marginal unit of the main

Oaxaquia orogen, that did not suffer the Zapotecan metamorphism (Figure 10a to 10e). Instead, a lower metamorphic grade, as that shown elsewhere by the *ca.* 940 Ma units which didn't undergo granulite metamorphism and were interpreted as outer units concerning the orogen core (Catalina Unit in Chiapas, Valencia-Morales *et al.*, 2022; Pochotepec suite in the Sierra de Juárez Complex, Espejo-Bautista *et al.*, 2023) would help to reconcile the absence of evident zircon recrystallization (concordia diagrams of Figures 4 and 5), with the clear metamorphic overprint that the Río Hondo metaigneous rocks suffered.

The discovery of the Río Hondo gneisses as an external Oaxaquia unit also has implications related to the Acatlán Complex formation and its tectonic juxtaposition against the Oaxacan Complex. These two concepts, described in recent years and several papers (*e.g.*, Elías-Herrera and Ortega-Gutiérrez, 2002; Elías-Herrera *et al.*, 2005; Keppie *et al.*, 2016 and 2018) will require further studies to be fully sustained. Our data point in indicating that the Río Hondo gneisses are, in fact, in tectonic contact with the Acatlán Complex along the Caltepec fault zone (and that they represent the protolith that undergoes partial melting to generate the Cozahuico granite and migmatites, *e.g.*, our sample MEH23-1). Furthermore, having similar TDM as the Oaxacan Complex, but a lower grade of metamorphism and more hydrated mineralogy than the Oaxacan Complex granulite they are, at least in principle, more fertile to generate granitic melts, such as the Ordovician granitoids widespread in the Acatlán Complex and studied by Keppie *et al.* (2018). These two hypotheses are compelling and will require further studies to be proven or discarded.
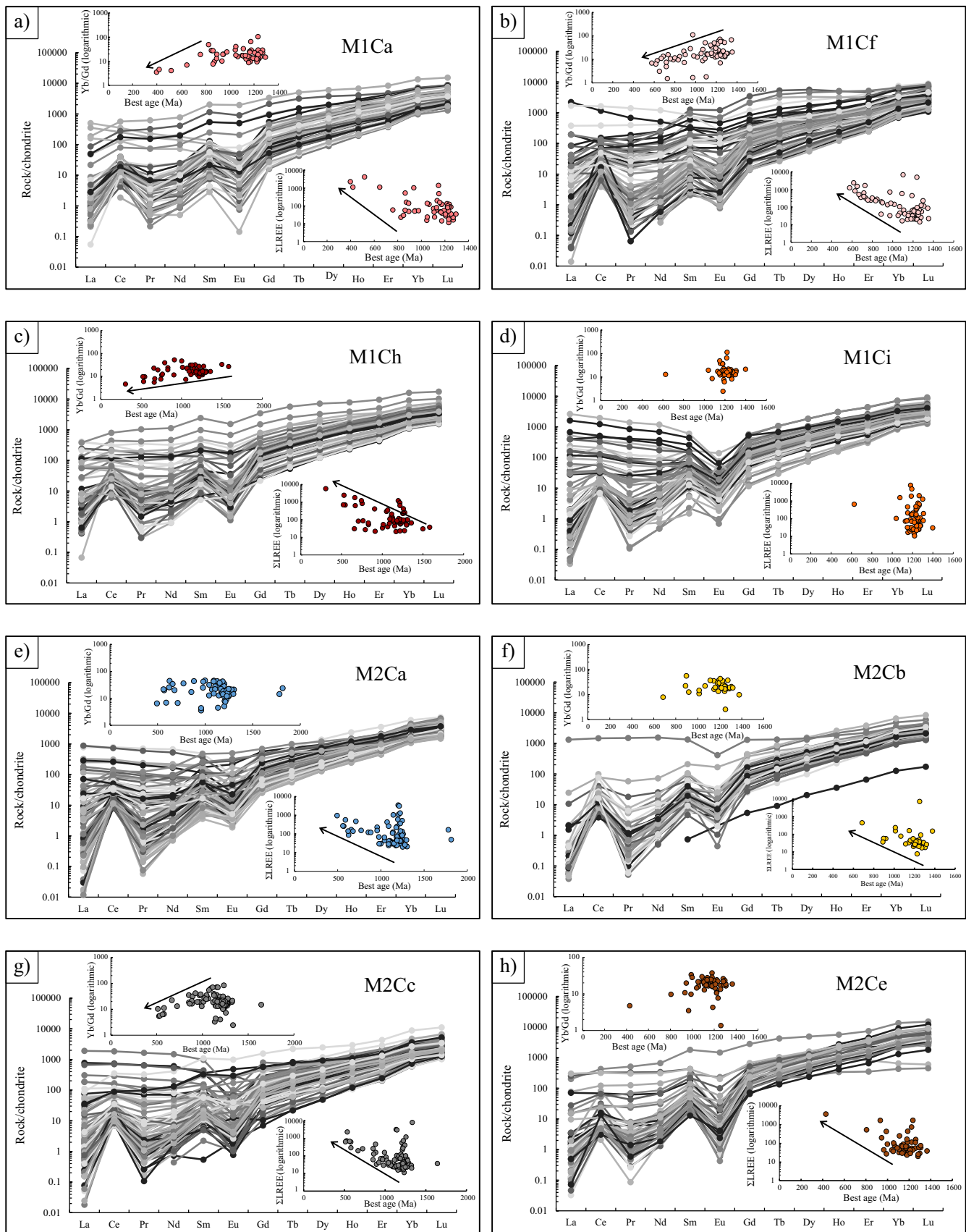
Figure 7. Chondrite-normalized REE analyses for the studied samples. Insets in each plot correspond to the variation of Yb/Gd and ΣLREE with age, respectively.

(continues).

Figure 7 (cont.). Chondrite-normalized REE analyses for the studied samples. Insets in each plot correspond to the variation of Yb/Gd and ΣLREE with age, respectively.
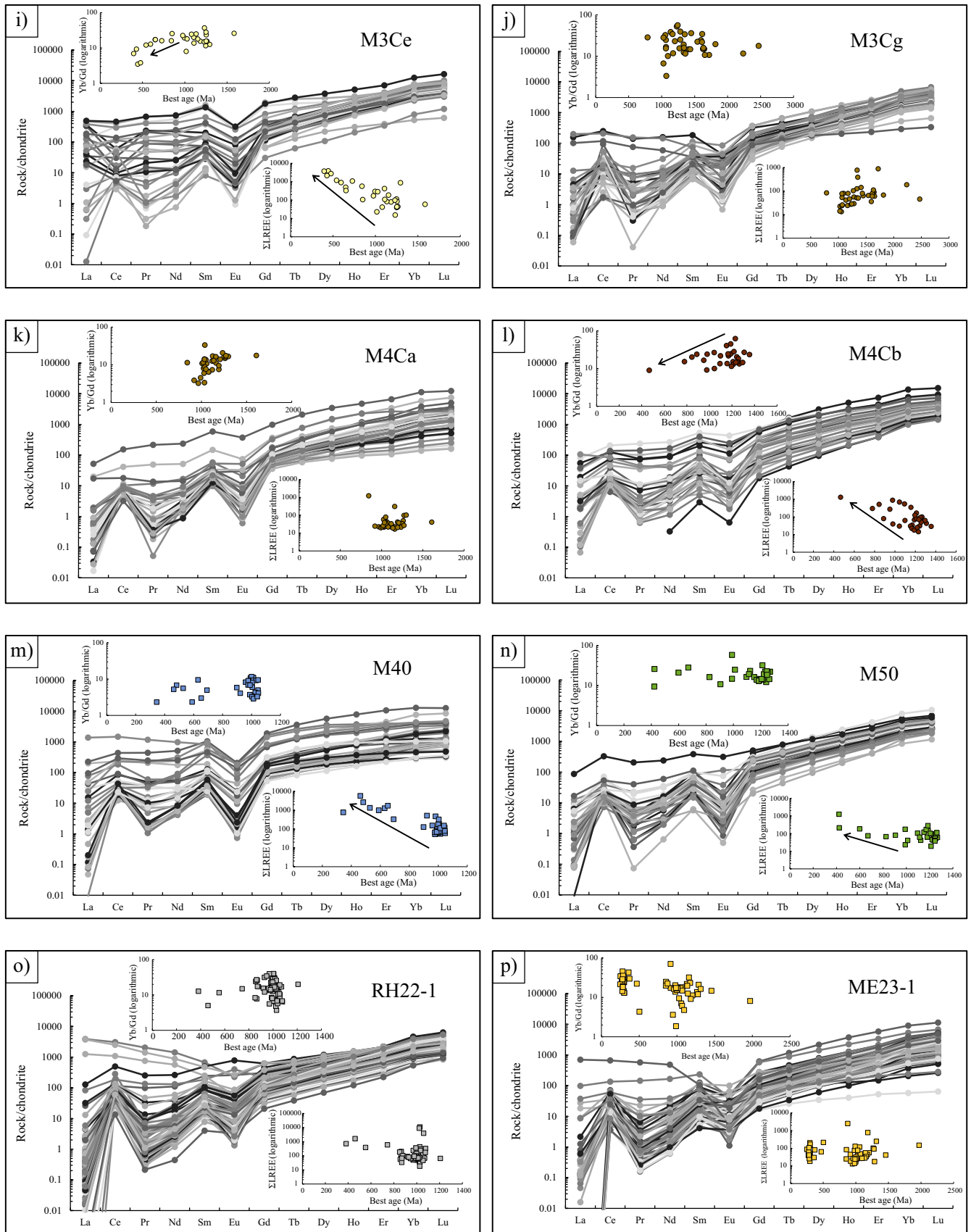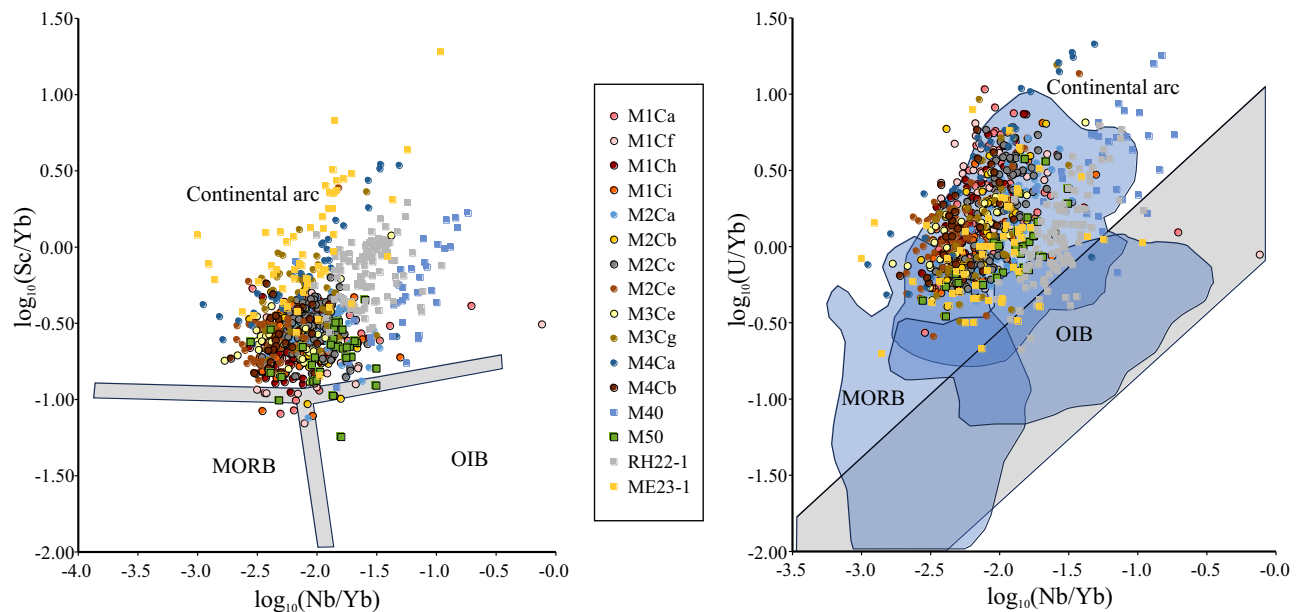
Figure 8. Sc/Yb *vs*. Nb/Yb and U/Yb *vs*. Nb/Yb discrimination diagrams for the zircon crystals analyzed in this work. In situ samples are represented by squared symbols, whereas clast samples with round ones. The continental arc, OIB and MORB fields, as well as the grey area representative of the mantle-zircon array, are from Grimes *et al.*, 2015.

CONCLUSIONS

The Río Hondo sequence consists of Mesoproterozoic (*ca.* 1200–1270 and *ca.* 1025 Ma) metaigneous rocks, metamorphosed under medium-grade conditions. Isotopically they resemble rocks elsewhere found in Oaxaquia (*e.g.*, the nearby Oaxacan Complex), with T_{DM} ages of *ca.* 1.5–1.65 Ga, and some minor reworked crustal

components of *ca.* 1.9 Ga. The absence of granulite-facies metamorphism, indicative of the Zapotecan event widespread in Oaxaquia, points toward an element that escaped those extreme metamorphic conditions. Although further studies are required to demonstrate its tectonic significance fully, we hypothesize that the Río Hondo sequence is directly related to the Paleozoic magmatic genesis of the Acatlán Complex.
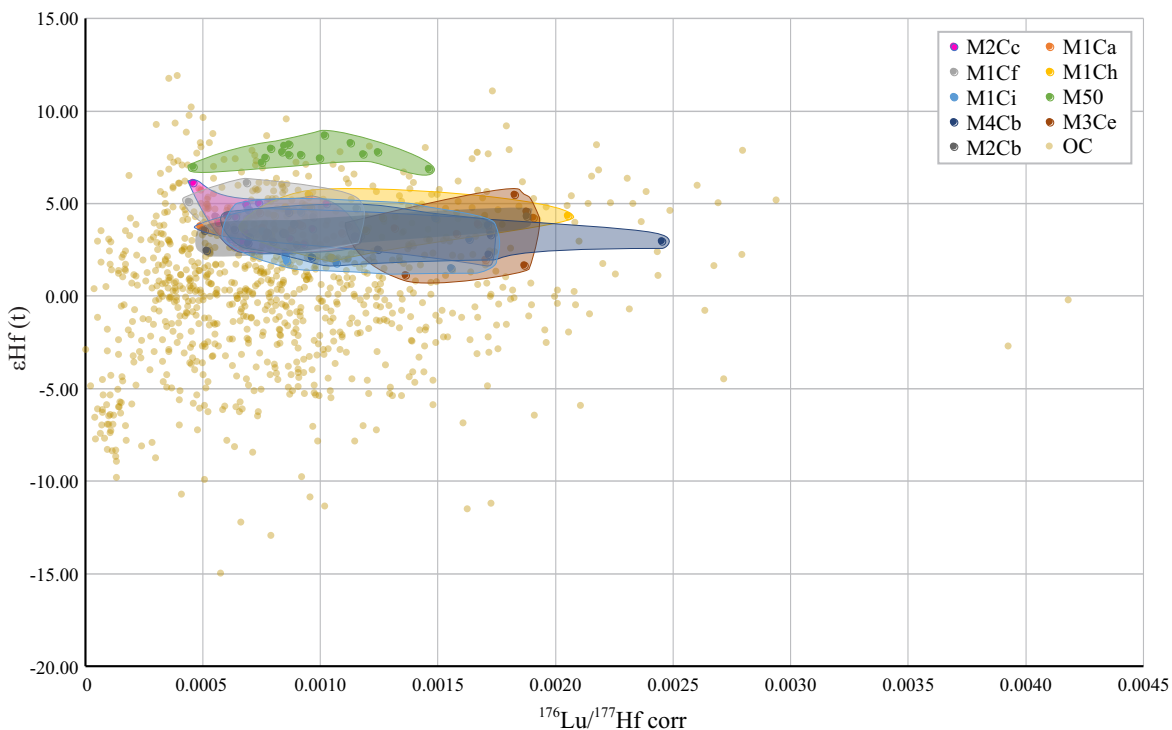

Figure 9. εHf *vs*. initial ^{176}Lu/^{177}Hf corrected ratios of the studied samples, compared with similar values of the Oaxacan Complex zircon grains obtained from Solari *et al.* (2020), light brown circles.

SUPPLEMENTARY MATERIAL

ACKNOWLEDGMENTS

REFERENCES

Adame-Martínez, M.G., Solari, L.A., Ortega-Obregón, C., Abdullin, F., 2020, U-Pb geochronology of rutile: deciphering the cooling history of the Oaxacan Complex granulites, southern Mexico: Revista Mexicana de Ciencias Geológicas, 37(2), 135-145, https://doi.org/10.22201/cgeo.20072902e.2020.2.1557.

Bahlburg, H., Vervoort, J.D., DuFrane, S.A., Carlotto, V., Reimann, C., Cardenas, J., 2011, The U–Pb and Hf isotope evidence of detrital zircons of the Ordovician Ollantaytambo Formation, southern Peru, and the Ordovician provenance and paleogeography of southern Peru and northern Bolivia: Journal of South American Earth Sciences, 32, 196-209, doi:10.1016/j.jsames.2011.07.002.

Bedoya, A., Anaya-Guarneros, J.A., Abdullin, F., Martini, M., Solari, L., 2021, Provenance analysis of the Matzitzi and Agua de Mezquite formations, southern Mexico: Different fluvial successions formed during late Paleozoic and post-Middle Jurassic time along the southernmost North America Pacific margin: Journal of South American Earth Sciences, 105, 102999.

Blichert-Toft, J., Albarède, F., 1997, The Lu–Hf isotope geochemistry of chondrites and the evolution of the mantle–crust system: Earth Planetary Science Letters, 148, 243-258.

Bouvier, A., Vervoort, J., Patchett, J., 2008, The Lu–Hf and Sm–Nd isotopic composition of CHUR: constraints from unequilibrated chondrites and implications for the bulk composition of terrestrial planets: Earth Planetary Science Letters, 273, 8-57.

Cameron, K., Lopez, R., Ortega-Gutiérrez, F., Solari, L., Keppie, J., Schulze, C., 2004, U-Pb geochronology and Pb isotopic compositions of leached feldspars: Constraints on the origin and evolution of Grenville rocks from eastern and southern Mexico, *in* Tollo, R.P., McClelland, J., Corriveau, L., Bartholomew, M.J., (eds.), Proterozoic Tectonic Evolution of the Grenville Orogen in North America: Geological Society of America Memoir, 197, 755-769, https://doi.org/10.1130/0-8137-1197-5.755.

Cawood, P.A., Hawkesworth, C.J., Dhuime, B., 2013, The continental record and the generation of continental crust: Geological Society of America Bulletin, 125, 14e32.

Centeno-García, E., Mendoza-Rosales, C.C., Silva-Romo, G., 2009, Sedimentología de la Formación Matzitzi (Paleozoico superior) y significado de sus componentes volcánicos, región de Los Reyes Metzontla-San Luis Atolotitlán, Estado de Puebla: Revista Mexicana de Ciencias Geológicas, 26, 18-36.

Chu, N., Taylor, R., Chavagnac, V., Nesbitt, R., Boella, R., Milton, J., German, C., Bayon, G., 2002, Hf isotope ratio analysis using multi-collector inductively coupled plasma mass spectrometry: an evaluation of isobaric interference corrections: Journal of Analytical Atomic Spectrometry, 17, 1567-1574. https://doi.org/10.1039/b206707b.

Elías-Herrera, M., Ortega-Gutiérrez, F., 2002, Caltepec fault zone: An Early Permian dextral transpressional boundary between the Proterozoic Oaxacan and Paleozoic Acatlán complexes, southern Mexico: Tectonics, 21-3, doi:10.1029/2000tc001278/full.

Elías-Herrera, M., Ortega-Gutiérrez, F., Sánchez-Zavala, J.L., Macías-Romo, C., Ortega-Rivera, A., Iriondo, A., 2005, La falla de Caltepec: raíces expuestas de una frontera tectónica de larga vida entre dos terrenos continentales del sur de México: Boletín de la Sociedad Geológica Mexicana, LVII, 83-109.

Elías-Herrera, M., Ortega-Gutiérrez, F., Macías-Romo, C., Sánchez-Zavala, J.L., Solari, L.A., 2011, Colisión oblicua del Cisuraliano-Guadalupiano entre bloques continentales en el sur de México: evidencias estratigráfico-estructurales y geocronológicas: Mexico City, Mexico, Instituto de Geología, Universidad Nacional Autónoma de México, Simposio Dr. Zoltan de Cserna: Sesenta años geologizando en México, Libro de Resúmenes, 159-164.

Espejo-Bautista, G., Solari, L., Maldonado, R., Ramírez-Calderón, M., 2023, Stenian arc- magmatism and early Tonian metamorphism and anatexis along the northern border of Amazonia during the Rodinia assembly: The Pochotepec suite in southern Mexico: Journal of South American Earth Sciences, 124, 104248.

Fisher, C.M., Hanchar, J.M., Samson, S.D., Dhuime, B., Blichert-Toft, J., Vervoort, J.D., Lam, R., 2011, Synthetic zircon doped with hafnium and rare earth elements: a reference material for in situ hafnium isotope analysis: Chemical Geology, 286, 1-2, 32-47, https//doi.org/10.1016/j.chemgeo.2011.04.013.

Fisher, C.M., Vervoort, J.D., Hanchar, J.M., 2014, Guidelines for reporting zircon Hf isotopic data by LA-MC-ICPMS and potential pitfalls in the interpretation of these data: Chemical Geology, 363, 125-133.

Gerdes, A., Zeh, A., 2009, Zircon formation versus zircon alteration — New insights from combined U–Pb and Lu–Hf *in-situ* LA-ICP-MS analyses, and consequences for the interpretation of Archean zircon from the Central Zone of the Limpopo Belt: Chemical Geology, 261, 230-243, https://doi.org/10.1016/j.chemgeo.2008.03.005.

Griffin, W.L., Wang, X., Jackson, S.E., Pearson, N.J., O'Reilly, S.Y., Xu, X., Zhou, X., 2002, Zircon chemistry and magma mixing, SE China: *in-situ* analysis of Hf isotopes, Tonglu and Pingtan igneous complexes: Lithos, 61, 237-269

Grimes, C.B., Wooden, J.L., Cheadle, M.J., John, B.E., 2015, "Fingerprinting" tectono- magmatic provenance using trace elements in igneous zircon: Contributions to Mineralogy and Petrology, 170, 1-26.

Harley, S.L., Kelly, N.M., Moeller, A., 2007, Zircon Behaviour and the Thermal Histories of Mountain Chains: Elements, 3, 1, 25-30, DOI:10.2113/gselements.3.1.25.

Hawkesworth, C.J., Kemp, A.I.S., 2006, Using hafnium and oxygen isotopes in zircons to unravel the record of crustal evolution: Chemical Geology, 226, 3-4, 144-162, https://doi.org/10.1016/j.chemgeo.2005.09.018.

Ibañez-Mejia, M., Pullen, A., Arenstein, J., Gehrels, G.E., Valley, J., Ducea, M.N., Mora, A.R., Pecha, M., Ruiz, J., 2015, Unraveling crustal growth and reworking processes in complex zircons from orogenic lower-crust: the Proterozoic Putumayo Orogen of Amazonia: Precambrian Research, 267, 285-310, doi:10.1016/j.precambres.2015.06.014.

Jaramillo-Jaramillo, M., 2020, Caracterización isotópica de los clastos metamórficos de los conglomerados basales de la Formación Matzitzi, Puebla y sus implicaciones tectónicas: Querétaro, Qro., Mexico, Universidad Nacional Autónoma de México, Posgrado en Ciencias de la Tierra, Centro de Geociencias, Tesis de Maestría, 152 pp.

Juárez-Zúñiga, S., Solari, LA, Ortega-Obregón, C., 2020, Permian igneous clasts from the Matzitzi Formation, southern Mexico: isotopic constraints on the final amalgamation of Pangaea, *in* Murphy, J.B., Strachan, R.A., Quesada, C. (eds), Pannotia to Pangaea: Neoproterozoic and Paleozoic Orogenic Cycles in the Circum-Atlantic Region: Geological Society, London, Special Publications, 503, doi:10.1144/SP503-2019-238.

Keppie, J.D., Dostal, J., 2007, Rift-related basalts in the 1.2–1.3 Ga granulites of the northern Oaxacan Complex, southern Mexico: Evidence for a rifted arc on the northwestern margin of Amazonia: Proceedings of the Geologists' Association, 118(1), 63-74, https://doi.org/10.1016/S0016-7878(07)80048-4.

Keppie, J.D., Dostal, J., Ortega-Gutierrez, F., Lopez, R., 2001, A Grenvillian arc on the margin of Amazonia: Evidence from the southern Oaxacan Complex, southern Mexico: Precambrian Research, 112, 165-181, https://doi.org/10.1016/S0301-9268(00)00150-9.

Keppie, J.D., Dostal, J., Cameron, K., Solari, L., Ortega-Gutiérrez, F., Lopez, R.L., 2003, Geochronology and geochemistry of Grenvillian igneous sui-

tes in the northern Oaxacan Complex, southern Mexico: Tectonic impli-
cations: Precambrian Research, 120, 365-389, https://doi.org/ 10.1016/
S0301-9268(02)00166-3.

Keppie, J.D., Dostal, J., Shellnutt, J.G., 2016, Old and juvenile source of Paleo-
zoic and Mesozoic basaltic magmas in the Acatlán and Ayú complexes,
Southern Mexico: Nd isotopic constraints: Tectonophysics, 681, 376-384.

Keppie, J. D., Dostal, J., Li, J., 2018, Nd isotopic data indicating Oaxacan source
of Ordovician granitoids in the Acatlán Complex, southern Mexico–Pa-
leogeographic implications: Tectonophysics, 740-741, 1-9, https://doi.
org/10.1016/j.tecto.2018.05.004.

Lawlor, P., Ortega-Gutiérrez, F., Cameron, K., Ochoa-Camarillo, H., Lopez, R.,
Sampson, D., 1999, U-Pb geochronology, geochemistry, and provenance
of the Grenvillian Huiznopala Gneiss of eastern Mexico: Precambrian Re-
search, 94, 1-2, 73-99, https://doi.org/10.1016/S0301-9268(98)00108-9.

Li, Z.X., Bogdanova, S.V., Collins, A.S., Davidson, A., De Waele, B., Ernst,
R.E., Fitzsimons, I.C.W., Ok, R.A., Gladkochub, D.P., Jacobs, J., Karls-
trom, K.E., Lu, S., Natapov, L.M., Pease, V., Pisarevsky, S.A., Thrane, K.,
Vernikovsky, V., 2008, Assembly, configuration, and break-up history of
Rodinia: A synthesis: Precambrian Research, 160, 1-2, 179-210, https://
doi.org/10.1016/j.precamres.2007.04.021.

Martini, M., Anaya-Guarneros, J.A., Solari, L.A., Bedoya-Mejía, A., Zepeda-
Martínez, M., Villanueva-Amadoz, U., 2022, The Matzitzi Formation in
southern Mexico A record of Pangea final assembly or breakup: Basin
Research 34, 727-747.

Mora, C., Valley, J., 1985, Ternary feldspar thermometry in granulites from the
Oaxacan Complex, Mexico: Contributions to Mineralogy and Petrology,
89, 215-225, https://doi.org/10.1007/BF00379455.

Ortega-Gutiérrez, F., Ruiz, J., Centeno-García, E., 1995, Oaxaquia, a Pro-
terozoic microcontinent accreted to North America during the late
Paleozoic: Geology, 23, 12, 1127-1130, https://doi.org/10.1130/0091-
7613(1995)023<1127:OAPMAT>2.3.CO;2.

Ortega-Gutiérrez, F., Elías-Herrera, M., Morán-Zenteno, D. J., Solari, L., We-
ber, B., Luna- González, L., 2018, The pre- Mesozoic metamorphic ba-
sement of Mexico, 1.5 billion years of crustal evolution: Earth-Science
Reviews, 183, 2-37, https://doi.org/10.1016/j.earsc irev.2018.03.006.

Ortega-Obregón, C., Solari, L., Gómez-Tuena, A., Elías-Herrera, M., Ortega-
Gutiérrez, F., Macías Romo, C., 2014, Permian–Carboniferous arc mag-
matism in southern Mexico: U–Pb dating, trace element and Hf isotopic
evidence on zircons of earliest subduction beneath the western margin
of Gondwana: International Journal of Earth Sciences, 103, 1287-1288,
https://doi.org/10.1007/s00531-013-0933-1.

Patchett, P.J., Tatsumoto, M., 1981, A routine high-precision method for Lu–
Hf isotope geochemistry and chronology: Contributions to Mineralogy
and Petrology, 75, 263-267.

Paton, C., Hellstrom, J., Paul, B., Woodhead, J., Hergt, J., 2011, Iolite: Freeware
for the visualisation and processing of mass spectrometric data: Journal
of Analytical Atomic Spectrometry, 26, 2508.

Payne, J.L., Pearson, N.J., Grant, K.J., Halverson, G.P., 2013, Reassessment
of relative oxide formation rates and molecular interferences on in situ
lutetium–hafnium analysis with laser ablation MC-ICP-MS: Journal of
Analytical Atomic Spectrometry, 28, 1068-1079.

Petrus, J.A., Kamber, B.S., 2012, VizualAge: a novel approach to laser abla-
tion ICP–MS U–Pb geochronology data reduction: Geostandards and
Geoanalytical Research, 36, 247-270, https://doi.org/10.1111/j.1751-
908X.2012.00158.x.

Scherer, E., Münker, C., Mezger, K., 2001, Calibration of the lutetium–haf-
nium clock: Science, 293, 683-687.

Sláma, J., Košler, J., Condon, D.J., Crowley, J.L., Gerdes, A., Hanchar, J.M.,
Horstwood, M.S.A., Morris, G.A., Nasdala, L., Norberg, N., Schaltegger,
U., Schoene, B., Tubrett, M.N., Whitehouse, M.J., 2008, Plešovice zircon
– a new natural reference material for U–Pb and Hf isotopic microa-
nalysis: Chemical Geology, 249, 1-35, https:// doi.org/10.1016/j.che-
mgeo.2007.11.005.

Solari, L.A., Keppie, J.D., Ortega-Gutiérrez, F., Cameron, K., Lopez, R., Ha-
mes, W.E., 2003, 990 and 1100 Ma Grenvillian tectonothermal events in
the northern Oaxacan Complex, southern Mexico: Roots of an orogeny:
Tectonophysics, 365(1-4), 257-282, https://doi.org/10.1016/ S0040-
1951(03)00025-8.

Solari, L.A., Keppie, J.D., Ortega-Gutiérrez, F., Cameron, K.L., López, R., 2004,
990 Ma peak granulitic metamorphism and amalgamation of Oaxaquia,

Mexico: U-Pb zircon geochronological and common Pb isotopic data:
Revista Mexicana de Ciencias Geológicas, 21(2), 212-225.

Solari, L., Torres de León, R., Hernandez Pineda, G., Sole, J., Solís-Pichardo,
G., Hernández-Treviño, T. 2007. Tectonic significance of Cretaceous Ter-
tiary magmatic and structural evolution of the northern margin of the
Xolapa Complex, Tierra Colorada area, southern Mexico: Bulletin of the
Geological Society of America, 119, 1265-1279, https://doi.org/10. 1130/
B26023.1.

Solari, L.A., Ortega-Gutiérrez, F., Elías-Herrera, M., Ortega-Obregón, C.,
Macías-Romo, C., Reyes Salas, M., 2014, Detrital provenance of the
Grenvillian Oaxacan Complex, southern Mexico: A zircon perspective:
International Journal of Earth Sciences, 103(5), 1301-1315, https://doi.
org/10.1007/s00531-013-0938-9.

Solari, L., González-León, C.M., Ortega-Obregón, C., Valencia-Moreno, M.,
Rascón-Heimpel, M.A., 2018, The Proterozoic of NW Mexico revisited:
U–Pb geochronology and Hf isotopes of Sonoran rocks and their tecto-
nic implications: International Journal of Earth Sciences, 107(3), 845-
861, 10.1007/s00531-017-1517-2.

Solari, L.A., Ortega-Obregón, C., Ortega-Gutiérrez, F., Elías-Herrera, M., 2021
Origin and evolution of the Grenvillian Oaxacan Complex, southern
Mexico: Hf isotopic and U-Pb geochronologic constraints, in Martens,
U., Molina Garza, R.S., (eds.), Southern and Central Mexico: Basement
Framework, Tectonic Evolution, and Provenance of Mesozoic–Cenozoic
Basins: Geological Society of America Special Paper, 546, 53-71, https://
doi.org/10.1130/2020.2546(03).

Valencia-Morales, Y. T., Weber, B., Tazzo-Rangel, M.D., González-Guzmán,
R., Frei, D., Quintana-Delgado, J.A., Rivera-Moreno, E.N., 2022, Early
Mesoproterozoic inliers in the Chiapas Massif Complex of southern
Mexico: Implications on Oaxaquia-Amazonia-Baltica configuration:
Precambrian Research, 373, 106611.

Vermeesch, P., 2018, IsoplotR: a free and open toolbox for geochronolo-
gy: Geoscience Frontiers, 9, 1479-1493, https://doi.org/10.1016/j.
gsf.2018.04.001.

Weber, R., 1997' How old is the Triassic flora of Sonora and Tamaulipas,
and news on Leonardian floras in Puebla and Hidalgo, México: Revista
Mexicana de Ciencias Geológicas, 14, 225-243.

Weber, B., Hecht, L., 2003, Petrology and geochemistry of metaigneous rocks
from a Grenvillian basement fragment in the Maya block: The Guichicovi
complex, Oaxaca, southern Mexico: Precambrian Research, 124(1),41-
67, https://doi.org/10.1016/S0301- 9268(03)00078-0.

Weber, B., Köhler, H., 1999, Sm-Nd, Rb-Sr and U-Pb geochronology of a
Grenville terrane in southern Mexico: Origin and geologic history of the
Guichicovi Complex: Precambrian Research, 96(3-4), 245-262, https://
doi.org/10.1016/S0301-9268(99)00012-1.

Weber, B., Schulze, C., 2014, Early Mesoproterozoic (>1.4 Ga) ages from
granulite basement inliers of SE Mexico and its implications on the
Oaxaquia concept—Evidence from U-Pb and Lu-Hf isotopes on zircon:
Revista Mexicana de Ciencias Geológicas, 31(3), 1-18.

Weber, B., Scherer, E.E., Schulze, C., Valencia, V.A., Montecinos, P., Mezger,
K., Ruiz, J., 2010, U-Pb and Lu-Hf isotope systematics of lower crust
from central-southern Mexico – Geodynamic significance of Oaxaquia
in a Rodinia realm: Precambrian Research, 182, (1-2), 149-162, https://
doi.org/10.1016/j.precamres.2010.07.007

Wiedenbeck, M., Allé, P., Corfu, F., Griffin, W.L., Meier, M., Oberli, F., Von
Quadt, A., Roddick, J., Spiegel, W., 1995, Three natural zircon standards
for U–Th–Pb, Lu–Hf, trace element and REE analyses: Geostandards
and Geoanalytical Research, 19, 1-23, https://doi.org/10.1111/j.1751-
908X.1995.tb00147.x

Woodhead, J., Hergt, J., Shelley, M., Eggins, S., Kemp, R., 2004, Zircon
Hf-isotope analysis with an excimer laser, depth profiling, ablation
of complex geometries, and concomitant age estimation: Chemical
Geology, 209, 121-135.

Zhong, S., Feng, C., Seltmann, R., Li, D., Qu, H., 2018, Can magmatic zircon be
distinguished from hydrothermal zircon by trace element composition?
The effect of mineral inclusions on zircon trace element composition:
Lithos, 314-315, 646-657.